3.3.2. Selection of phosphate contribution

Phosphate ions lead to various FTIR contributions. However, since the $\nu_1(PO_4)$ and $\nu_2(PO_4)$ modes are only poorly active in infrared, considering them for quantification purposes would lead to increased uncertainties. In contrast, the $\nu_3(PO_4)$ and $\nu_4(PO_4)$ domains are significantly more intense, which is expected to limit propagated errors. The libration band of apatitic OH^- ions, however, appears at 632 cm^{-1}, which superimposes to the $\nu_4(PO_4)$ domain. Since apatite compounds are often nonstoichiometric due to the presence of vacancies in calcium and hydroxide sites, the level of hydroxylation may significantly vary from one sample to another, thus modifying the overall shape of the $\nu_4(PO_4)$ band. As this libration contribution can be non-negligible in intensity but also because it cannot easily be distinguished from the phosphate vibrations belonging to the $\nu_4(PO_4)$ domain (unless using time-consuming spectral decomposition methods), the exploration of the $\nu_4(PO_4)$ domain for in carbonate quantification methodology does not seem appropriate.

Overall, the $\nu_3(PO_4)$ appears the best choice to assess carbonate contents of apatite. However, especially in low-crystallinity samples, the $\nu_1(PO_4)$ singlet vibration is not cleanly separated from the $\nu_3(PO_4)$ band (e.g. Fig. 2b), and appears as a shoulder to $\nu_1(PO_4)$. Thus the combined $\nu_1\nu_3(PO_4)$ domain appears most practical in avoiding additional spectral treatment to subtract the $\nu_1(PO_4)$ contribution.

3.4. Exploration of FTIR methodologies

The vibrational domains retained for this carbonation analysis are $\nu_3(CO_3)$ for carbonate ions and $\nu_1\nu_3(PO_4)$ for phosphates. Based on our experimental IR spectra, we measured for each of the reference samples, using the OMNIC 8 software, the integrated intensities (=peak areas) corresponding to these three components. These measurements were carried out after a preliminary baseline correction of the complete 4000–400 cm^{-1} spectrum. The integration of the $\nu_3(CO_3)$ band was done in such a way as to include the totality of the $\nu_3(CO_3)$ contribution, typically between 1570 and 1330 cm^{-1}. The $\nu_1\nu_3(PO_4)$ contribution was integrated between 1230 and ~900 cm^{-1}. This lower limit was selected as the local minimum in order to avoid including the band expanding from *ca.* 800 to *ca.* 900 cm^{-1} due to $\nu_2(CO_3)$ and to HPO_4^{2-}. The upper limit of 1230 cm^{-1} was chosen because collagen subtraction for biological samples is bound to alter the region 1930–1230 cm^{-1} where amide bands are located (Boskey et al., 2005). The evaluation of the band area corresponding to $\nu_1\nu_3(PO_4)$ was found, in contrast, to be essentially unaffected (data not presented graphically here) by the collagen subtraction between these limits of 1230 and 900 cm^{-1}, therefore confirming the possibility of using this wavenumber range. The integration areas of interest for the determination of the carbonate/phosphate ratio denoted "$r_{c/p}$" between the integrated intensity of $\nu_3(CO_3)$ and that of $\nu_1\nu_3(PO_4)$ are shown graphically in Fig. 4a.

The evolution of the amount of carbonate in reference samples (as measured by coulometry) has been plotted in Fig. 4b versus the ratio $r_{c/p}$. Interestingly, a linear trend could be evidenced (see raw data on Table AR1 in the Additional Resources), with good correlation parameters ($R^2 = 0.985$), leading to the relationship given in Equation (1):

$$\text{wt.\% } CO_3 = 28.62 * r_{c/p} + 0.0843 \quad (1)$$

Despite absolute uncertainties on data points, this correlation confirms advantageously the possibility to exploit IR data for drawing quantitative assessments on the level of carbonation of apatitic compounds, and using the areas of the two spectral components $\nu_3(CO_3)$ and $\nu_1\nu_3(PO_4)$. The ordinate values (y-axis) given by this method are associated with an absolute error close to ±0.5% on the final wt.% CO_3. In this Figure, the fitted line was graphically prolonged (dashed line) down to 2 wt.% CO_3 and up to 13 wt.% CO_3 to access visually the correspondence between $r_{c/p}$ and wt.% CO_3 for a larger range of carbonation levels.

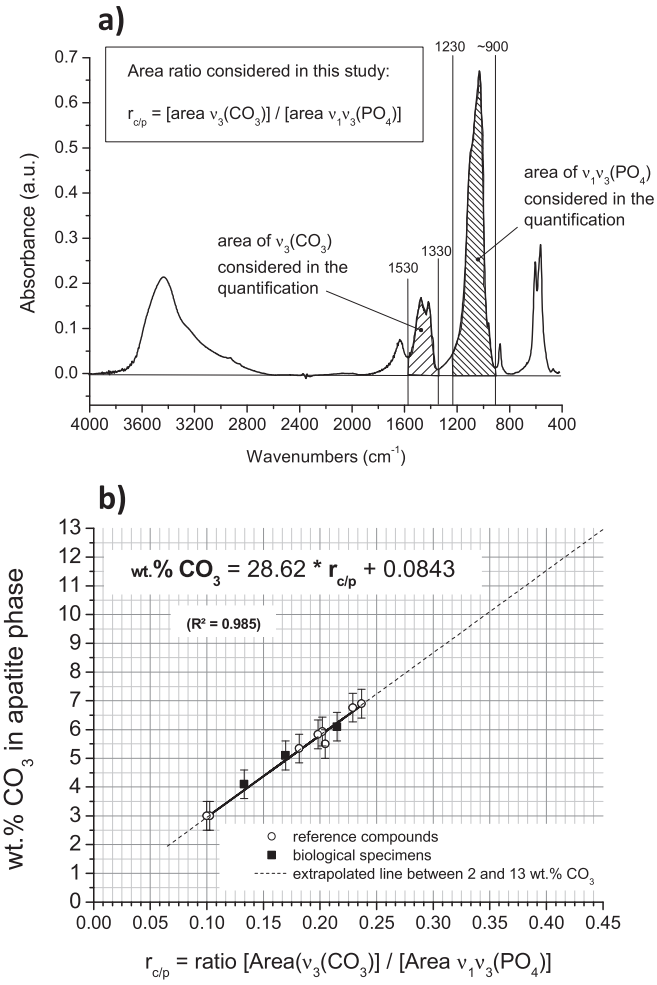

Fig. 4. FTIR methodology for carbonate quantification: a) evaluation of the ratio $r_{c/p}$ between the integrated intensity of $\nu_3(CO_3)$ and that of $\nu_1\nu_3(PO_4)$, and b) correlation between $r_{c/p}$ and the carbonation amount (in wt.% CO_3) in the apatite phase of synthetic reference compounds and for three biological samples.

If the same type of relationship is sought by considering the $\nu_4(PO_4)$ domain instead of $\nu_1\nu_3(PO_4)$, a poorer correlation is reached: when applied to reference samples from Table 1, a correlation coefficient of R^2 ~ 0.82 is found (see Fig. AR2 in the Additional Resources). This poor agreement was expected based on the above discussion (see previous section), because the level of hydroxylation of the apatite phase is bound to vary between samples, and the $\nu_{lib}(OH)$ libration band at 632 cm^{-1} cannot be easily separated from the large $\nu_4(PO_4)$ band, therefore generating a bias to the use of the $\nu_4(PO_4)$ band in the determination of a carbonation ratio.

If $r_{c/p}$ is calculated by considering the area of the $\nu_2(CO_3)$ band instead of $\nu_3(CO_3)$, an even poorer correlation is observed with the amount of carbonate of the reference compounds, with a coefficient of R^2 ~ 0.46 (Fig. AR2). Again, this illustrates the inadequacy mentioned in the previous section to inspect the carbonation level on the basis of the $\nu_2(CO_3)$ band, which in fact also contains a non-negligible and varying HPO_4 contribution among the samples.

As indicated in the introduction, the use of peak heights rather than areas has been proposed to follow the carbonation level of apatites, especially by considering the maximum at 1415 cm^{-1} (in the $\nu_3(CO_3)$ domain) relative to the phosphate maximum of the $\nu_3(PO_4)$ band, around 1040 cm^{-1} (exact position depending on the samples). Plotting the carbonate content measured by coulometry versus this height ratio led, when applied to the reference samples, to a correlation coefficient of R^2 ~0.76 (Fig. AR2). Although a rather linear trend can be observed here, the quality of this correlation remains lower than the one obtained using the $r_{c/p}$ area ratio (R^2 ~ 0.99).

All of these findings validate the $r_{c/p}$ area ratio between $\nu_3(CO_3)$ and $\nu_1\nu_3(PO_4)$ as the most adapted FTIR parameter to consider for carbonation quantification in apatites, this ratio being defined as the quotient between the full area of the $\nu_3(CO_3)$ band (typically in the range 1570–1330 cm^{-1}) and the area of the $\nu_1\nu_3(PO_4)$ band (typically in the range 900–1230 cm^{-1}).

At this point, it was interesting to check the validity of this $\%CO_3 = f(r_{c/p})$ relationship also for biological apatites. Three skeletal specimens (two from bones and one from a tooth), as described in the experimental section, were selected to this end. The absence of calcite as secondary deposit in these biological/fossil specimens was confirmed by XRD analyses as well as IR spectroscopy (absence of the calcite band at 712 cm^{-1}). In a first step, the carbonation of each of these three samples was directly measured by coulometry. This was made possible by the occurrence of enough bone/tooth matter for the selected specimens, as 50–80 mg of sample was needed in each coulometry experiment (performed at least in duplicate). As always for coulometry assays, a calibration was preliminarily done with barium carbonate ($BaCO_3$). Since skeletal specimens are also associated with an organic matrix, most of which is collagenic in nature, we also ran a test with a known quantity of $BaCO_3$ added with bovine collagen (type I from bovine Achilles tendon, Sigma Aldrich), 12 wt.% in proportion, in order to check whether the presence of this protein in the reacting cell could modify the response of the coulometer. Advantageously, no deviation of the apparatus outcome was pointed out, confirming that coulometry assays could also be run on biological specimens. Considering bone and tooth samples as containing respectively 20 and ~5% of organic matter, the coulometry results (obtained initially with 50–80 mg of bone/tooth specimen) could be corrected to derive the amount of carbonation relative to the mineral phase (apatite only) in these samples. This led to a carbonation level in the apatite phase contained in the biological samples "20th Cent", "mid-ages", and "Iron age" of wt.% CO_3 = 5.1, 4.1, and 6.1% (±0.5%), respectively.

In addition, FTIR spectra were collected for these three skeletal specimens, in the same conditions as was done above for synthetic reference compounds. Fig. 5 reports a typical example obtained for such biological specimens. Due to the presence of the organic matrix, the spectral signature of collagen appears clearly on the spectrum with amide bands distinguishable in the region of 1930–1230 cm^{-1}, thus partly overlapping with inorganic carbonate. In order to take into account, in the $\%CO_3 = f(r_{c/p})$ relationship, only the vibrational contribution of carbonate, a spectral treatment was carried out by subtracting a typical spectrum of type I bovine bone collagen (modern collagen from own collection; access to IR spectra for collagen with varying preservation states in link with diagenesis were not accessible to us) until minimizing the amide contributions in the above-cited region (Fig. 5). In practice, this subtraction of the collagen contribution thus consisted in increasing the multiplying factor "γ" in the global equation [corrected spectrum] = [initial spectrum] − γ*[collagen spectrum] until obtaining visually a negligible absorption for the amide contributions. This collagen subtraction resulted in spectra judged

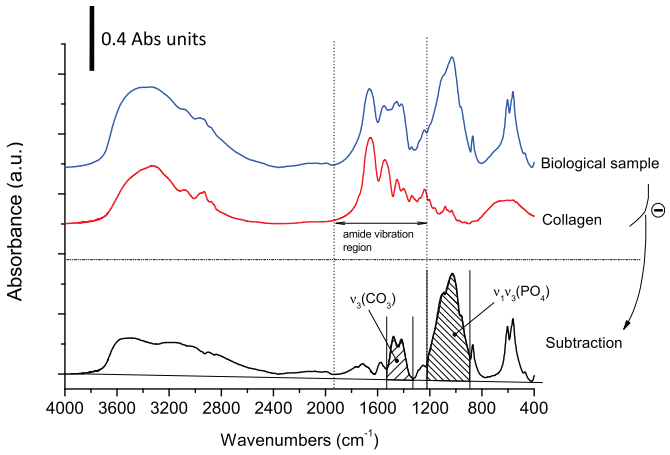

Fig. 5. Example of FTIR spectrum for biological specimen (case of Iron age bone sample) and for collagen (modern bovine bone collagen type I from own collection), and subtraction result (obtained by minimizing the intensity of amide vibrations in the 1930–1230 cm^{-1} domain).

satisfactory in terms of global appearance as compared with usual FTIR data recorded for synthetic carbonated apatites (see Fig. 2). Notably, the $\nu_1\nu_3(PO_4)$ domain was found to be only affected around the base of the absorption band without noticeable alteration of its general shape, thus making it potentially usable for quantification purposes. It may be noted that non-collagenous residues may also be present in biological/fossil specimens, however their amounts remain limited as compared to that of collagen. By analyzing by FTIR the organic residue found after acidic dissolution of the apatite mineral, we confirmed for the samples studied here that collagen was main organic component, and that non-collagenous matter led to very minor modifications of the 1530–1330 cm^{-1} carbonate domain (Fig. AR3 in the Additional Resources).

After collagen subtraction, the integrated intensities of the full $\nu_3(CO_3)$ domain (range 1530–1330 cm^{-1}) and of the $\nu_3\nu_1(PO_4)$ band (between 1230 and 890 cm^{-1}) were measured as done previously for synthetic samples, allowing us to derive the corresponding $r_{c/p}$ ratios. The application of Equation (1) to these data led to the respective carbonate contents of 4.9 ± 0.5, 3.9 ± 0.5 and 5.7 ± 0.5%, for samples "20th Cent", "mid-ages", and "Iron age" (to be compared with 5.1 ± 0.5, 4.1 ± 0.5 and 6.1 ± 0.5). A good agreement is, therefore, found between estimated carbonate contents calculated from Equation (1) and coulometric data for these biological samples. The three datapoints corresponding to these biological specimens have been added to the $\%CO_3 = f(r_{c/p})$ plot in Fig. 4b, which shows graphically that the IR-based methodology described in this paper for the quantification of carbonation of apatite phases is also applicable to skeletal specimens, provided that the vibrational contribution of collagen is preliminarily subtracted.

4. Concluding statements

The question of carbonate quantification in apatitic compounds, whether of synthetic or biological origin, is relevant for many reasons. In synthetic systems, the determination of the level of carbonation allows to draw conclusions relative to the degree of "biomimetism" of the sample, for example, as compared with mature or newly-formed bone matter. The presence of carbonation ions can clearly influence crystallization processes and these ions may also stabilize the non-apatitic surface layer on apatitic nanocrystals. Synthetic carbonated apatites could also serve as reference materials in view of the establishment of calibration curves, for example, in relation to biogenic phosphates that may have been

formed at various temperatures. In this contribution, we noted the direct effect of synthesis temperature on the level of carbonation and on other parameters such as crystallinity, evidenced on the basis of FTIR spectral analysis. In the case of skeletal specimens, the exploration of the carbonate content is of prime importance for characterizing these samples and drawing conclusions on biomineralization, diagenetic evolutions, paleoecology, etc., especially by exploiting ^{13}C and ^{18}O isotopic responses.

In this contribution, based on FTIR data, we discussed which carbonate and phosphate vibrations bands appear the most appropriate for carbonation quantification. We then developed and tested a quantification methodology based on an area ratio between the $\nu_3(CO_3)$ band and the $\nu_1\nu_3(PO_4)$ contribution, with integration limits that have been defined. We also checked this methodology quantitatively in comparison with direct coulometry measurements performed both on synthetic reference samples ($R^2 = 0.985$) and biological/fossil specimens, pointing out a good overall correlation. The absence of carbonated secondary deposits such as calcite should be verified for fossil specimens, for instance on the basis of XRD and/or IR analyses (e.g. absence of sharp band at 712 cm^{-1}).

The obtained relationship, expressed by Equation (1) (wt.% $CO_3 = 28.62^{*}r_{c/p} + 0.0843$), is intended to serve in the future for more systematic and comparable studies dedicated to carbonated apatites, whether of synthetic or natural origin.

Acknowledgments

This research was supported in part by the Institute of Ecology and Environment (INEE) and the Institute of Chemistry (INC) of the French National Center for Scientific Research (CNRS).

Appendix A. Supplementary data

Supplementary data related to this article can be found at http://dx.doi.org/10.1016/j.jas.2014.05.004.

References

Boskey, A.L., DiCarlo, E., Paschalis, E., West, P., Mendelsohn, R., 2005. Comparison of mineral quality and quantity in iliac crest biopsies from high- and low-turnover osteoporosis: an FT-IR microspectroscopic investigation. Osteoporos. Int. 16 (12), 2031–2038.

Cazalbou, S., Eichert, D., Drouet, C., Combes, C., Rey, C., 2004. Biological mineralisations based on calcium phosphate. Comptes. Rendus. Palevol. 3 (6–7), 563–572.

Drouet, C., 2013. Apatite formation: why it may not work as planned, and how to conclusively identify apatite compounds. Biomed. Res. Int. 2013, 12 http://dx.doi.org/10.1155/2013/490946. Article ID 490946.

Eichert, D., Drouet, C., Sfihi, H., Rey, C., Combes, C., 2007. Nanocrystalline apatite-based biomaterials: synthesis, processing and characterization. In: Kendall, J.B. (Ed.), Biomaterials Research Advances. Nova Science Publishers, pp. 93–143.

Elliott, J.C., 1994. Structure and Chemistry of the Apatites and Other Calcium Orthophosphates, vol. 18. Elsevier Science, Amsterdam.

Elliott, J.C., Holcomb, D.W., Young, R.A., 1985. Infrared determination of the degree of substitution of hydroxyl by carbonate ions in human dental enamel. Calcif. Tissue Int. 37 (4), 372–375.

Engleman, E.E., Jackson, L.L., Norton, D.R., 1985. Determination of carbonate carbon in geological materials by coulometric titration. Chem. Geol. 53 (1–2), 125–128.

Featherstone, J.D.B., Pearson, S., Legeros, R.Z., 1984. An infrared method for quantification of carbonate in carbonated apatites. Caries Res. 18 (1), 63–66.

Gee, A., Dietz, V.R., 1953. Determination of phosphate by differential spectrophotometry. Ann. Chem. 25, 1320–1324.

Gomez-Morales, J., Iafisco, M., Manuel Delgado-Lopez, J., Sarda, S., Drouet, C., 2013. Progress on the preparation of nanocrystalline apatites and surface characterization: overview of fundamental and applied aspects. Prog. Cryst. Growth Charact. Mater. 59 (1), 1–46.

Grunenwald, A., Keyser, C., Sautereau, A.M., Crubezy, E., Ludes, B., Drouet, C., 2014. Adsorption of DNA on biomimetic apatites: toward the understanding of the role of bone and tooth mineral on the preservation of ancient DNA. Appl. Surf. Sci. 292, 867–875.

Huffman, E.W.D., 1977. Performance of a new automatic carbon-dioxide coulometer. Microchem. J. 22 (4), 567–573.

Kimura-Suda, H., Kajiwara, M., Matsumoto, N., Murayama, H., Yamato, H., 2009. Characterization of apatite and collagen in bone with FTIR imaging. Mol. Cryst. Liq. Cryst. 505, 302–307.

Kohn, M.J., Schoeninger, M.J., Barker, W.W., 1999. Altered states: effects of diagenesis on fossil tooth chemistry. Geochim. Et. Cosmochim. Acta 63 (18), 2737–2747.

Kohn, M.J., Schoeninger, M.J., Valley, J.W., 1996. Herbivore tooth oxygen isotope compositions: effects of diet and physiology. Geochim. Et. Cosmochim. Acta 60 (20), 3889–3896.

Landis, W.J., Hodgens, K.J., Arena, J., Song, M.J., McEwen, B.F., 1996. Structural relations between collagen and mineral in bone as determined by high voltage electron microscopic tomography. Microsc. Res. Tech. 33 (2), 192–202.

Lebon, M., Müller, K., Bellot-Gurlet, L., Paris, C., Reiche, I., 2011. Application des micro-spectrométries infrarouge et Raman à l'étude des processus diagénétiques altérant les ossements paléolithiques. ArchéoSciences 35, 179–190.

Lecuyer, C., Balter, V., Martineau, F., Fourel, F., Bernard, A., Amiot, R., Gardien, V., Otero, O., Legendre, S., Panczer, G., Simon, L., Martini, R., 2010. Oxygen isotope fractionation between apatite-bound carbonate and water determined from controlled experiments with synthetic apatites precipitated at 10-37 degrees C. Geochim. Et. Cosmochim. Acta 74 (7), 2072–2081.

Legros, R., Balmain, N., Bonel, G., 1987. Age-related changes in mineral of rat and bovine cortical bone. Calcif. Tissue Int. 41 (3), 137–144.

McElderry, J.D.P., Zhu, P.Z., Mroue, K.H., Xu, J.D., Pavan, B., Fang, M., Zhao, G.S., McNerny, E., Kohn, D.H., Franceschi, R.T., Holl, M.M.B., Tecklenburg, M.M.J., Ramamoorthy, A., Morris, M.D., 2013. Crystallinity and compositional changes in carbonated apatites: evidence from P-31 solid-state NMR, Raman, and AFM analysis. J. Solid State Chem. 206, 192–198.

Pasteris, J.D., Yoder, C.H., Wopenka, B., 2014. Molecular water in nominally unhydrated carbonated hydroxylapatite: the key to a better understanding of bone mineral. Am. Mineralogist 99 (1), 16–27.

Pellegrino, E.D., Biltz, R.M., 1972. Mineralization in the chick embryo. I. Monohydrogen phosphate and carbonate relationships during maturation of the bone crystal complex. Calcif. Tissue Res. 10 (2), 128–135.

Price, T.D., Schoeninger, M.J., Armelagos, G.J., 1985. Bone chemistry and past behavior – an overview. J. Hum. Evol. 14 (5), 419–447.

Puceat, E., Reynard, B., Lecuyer, C., 2004. Can crystallinity be used to determine the degree of chemical alteration of biogenic apatites? Chem. Geol. 205 (1–2), 83–97.

Rey, C., Collins, B., Goehl, T., Dickson, I.R., Glimcher, M.J., 1989. The carbonate environment in bone-mineral – a resolution enhanced Fourier-Transform Infrared-Spectroscopy study. Calcif. Tissue Int. 45 (3), 157–164.

Rey, C., Combes, C., Christophe, D., Grossin, D., 2011. Bioactive ceramics: physical chemistry. In: Ducheyne, P., Healy, K.E., Hutmacher, D.W., Grainger, D.W., Kirkpatrick, C.J. (Eds.), Comprehensive Biomaterials. Elsevier, pp. 187–221.

Roche, D., Segalen, L., Balan, E., Delattre, S., 2010. Preservation assessment of Miocene–Pliocene tooth enamel from Tugen Hills (Kenyan Rift Valley) through FTIR, chemical and stable-isotope analyses. J. Archaeol. Sci. 37 (7), 1690–1699.

Shemesh, A., 1990. Crystallinity and diagenesis of sedimentary apatites. Geochim. Cosmochim. Acta 54 (9), 2433–2438.

Shimoda, S., Aoba, T., Moreno, E.C., Miake, Y., 1990. Effect of solution composition on morphological and structural features of carbonated calcium apatites. J. Dent. Res. 69 (11), 1731–1740.

Sosa, C., Vispe, E., Nunez, C., Baeta, M., Casalod, Y., Bolea, M., Hedges, R.E.M., Martinez-Jarreta, B., 2013. Association between ancient bone preservation and DNA Yield: a multidisciplinary approach. Am. J. Phys. Anthropol. 151 (1), 102–109.

Sponheimer, M., Lee-Thorp, J.A., 2001. The oxygen isotope composition of mammalian enamel carbonate from Morea Estate, South Africa. Oecologia 126 (2), 153–157.

Suarez, C., Kohn, M., 2011. Does carbonate content of biogenic apatite correlate with body temperature? J. Vertebrate Paleontol. 31, 201–201.

Termine, J.D., Posner, A.S., 1966. Infra-ref determination of the percentage of crystallinity in apatitic calcium phosphates. Nature 211, 268–270.

Thompson, T.J.U., Islam, M., Piduru, K., Marcel, A., 2011. An investigation into the internal and external variables acting on crystallinity index using Fourier Transform Infrared Spectroscopy on unaltered and burned bone. Palaeogeogr. Palaeoclimatol. Palaeoecol. 299 (1–2), 168–174.

Trueman, C.N., Privat, K., Field, J., 2008. Why do crystallinity values fail to predict the extent of diagenetic alteration of bone mineral? Palaeogeogr. Palaeoclimatol. Palaeoecol. 266 (3–4), 160–167.

Tütken, T., Vennemann, T.W., 2011. Fossil bones and teeth: preservation or alteration of biogenic compositions? Palaeogeogr. Palaeoclimatol. Palaeoecol. 310 (1–2), 1–8.

Vandecandelaere, N., Rey, C., Drouet, C., 2012. Biomimetic apatite-based biomaterials: on the critical impact of synthesis and post-synthesis parameters. J. Mater. Sci. Mater. Med. 23 (11), 2593–2606.

Weiner, S., Bar-Yosef, O., 1990. States of preservation of bones from prehistoric sites in the near east: a survey. J. Archaeol. Sci. 17 (2), 187–196.

Weiner, S., Wagner, H.D., 1998. The material bone: structure mechanical function relations. Annu. Rev. Mater. Sci. 28, 271–298.